COMPARATIVE ANALYSIS OF MODELS FOR ELASTIC pp SCATTERING*

E. Ferreira, T. Kodama, A.K. Kohara, D. Szilard

Instituto de Física, Universidade Federal do Rio de Janeiro
Caixa Postal 68528, 21945-970 Rio de Janeiro, Rio de Janeiro, Brazil

(Received November 12, 2015)

Three models for the $|t|$-dependence of the amplitudes in pp elastic scattering are reviewed with comparison of their similarities and differences.

DOI:10.5506/APhysPolBSupp.8.1017
PACS numbers: 13.85.Dz, 13.85.Lg

1. Introduction

The description of hadronic elastic scattering in terms of fundamentals of QCD remains an open problem. It involves non-perturbative aspects of strong interactions and may lead to a deeper comprehension of QCD interactions and hadronic structure. In the absence of theoretical solutions for the non-linear dynamics, the treatment depends on models. The interest in this problem is renewed due to the high-energy data from TOTEM [1] and ATLAS [2] experiments at the LHC.

The description of the pp (or $p\bar{p}$) cross section in a complete t-range depends on the interplay of the imaginary and real parts of the scattering amplitudes. In the present work, the attention is given to models where the description of the pp high-energy scattering through amplitudes is explicit. We concentrate on three models of this kind.

In Sections 2, 3 and 4, three models, here called KFK, BSW and HEGS, are summarized. In Section 5, we compare some of their features and present some comments.

2. KFK model

The KFK (short for Kohara–Ferreira–Kodama) model, inspired by the Stochastic Vacuum Model [3], has been successfully applied to $d\sigma/dt$ data from $\sqrt{s} \sim 20$ GeV to 7 TeV [4, 5].

* Presented at EDS Blois 2015: The 16th Conference on Elastic and Diffractive Scattering, Borgo, Corsica, France, June 29–July 4, 2015.

The amplitudes $T_K(s,t)$ are built based on the profile functions in the impact parameter representation

$$\tilde{T}_K(s,b) = \frac{\alpha_K(s)}{2\,\beta_K(s)}\, e^{-b^2/4\beta_K(s)} + \lambda_K(s)\,\tilde{\psi}(s,b) \tag{1}$$

with the characteristic shape function

$$\tilde{\psi}_K(s,b) = \frac{2\, e^{\gamma_K(s)-\sqrt{\gamma_K(s)+b^2/a_0}}}{a_0\sqrt{\gamma_K(s)+b^2/a_0}} \left[1 - e^{\gamma_K(s)-\sqrt{\gamma_K(s)+b^2/a_0}}\right], \tag{2}$$

where $K = R, I$ labels the real and the imaginary parts of the amplitude; $a_0 = 1.39$ GeV^{-2} is related to the gluon correlation length of the correlation function. The Fourier transform of Eq. (1) determines the real and imaginary scattering amplitude in t-space

$$T_K(s,t) = \frac{1}{2\pi}\int_0^\infty d^2\vec{b}\, e^{-i\vec{q}\cdot\vec{b}}\,\tilde{T}_K(s,b) \tag{3}$$

with $t = -\vec{q}^{\,2}$. A characteristic feature of this model is that the amplitudes in both b- and t-space have simple analytical forms, mathematically related. The real and imaginary amplitude in t-space are written

$$T_K(s,t) = \alpha_K(s)\, e^{-\beta_K|t|} + \lambda_K(s)\,\Psi_K(\gamma_K(s),t) + \delta_{K,R}\, R_{ggg}(t)\,. \tag{4}$$

We have now added the term $R_{ggg}(t)$ that represents the contribution from the perturbative three-gluon exchange and is responsible for the observed $|t|^{-8}$ tail behaviour [6] in $d\sigma/dt$. The shape functions in t-space are

$$\Psi_K(\gamma_K(s),t) = 2e^{\gamma_K}\left[\frac{e^{-\gamma_K\sqrt{1+a_0|t|}}}{\sqrt{1+a_0|t|}} - e^{\gamma_K}\frac{e^{-\gamma_K\sqrt{4+a_0|t|}}}{\sqrt{4+a_0|t|}}\right]. \tag{5}$$

The KFK model uses four energy-dependent parameters for each amplitude, $\alpha_K(s)$, $\beta_K(s)$, $\lambda_K(s)$ and $\gamma_K(s)$. The energy dependence of the parameters is given in [5]. Here, we are concerned only with pp scattering at high energies.

3. BSW model

The BSW model was formulated more than thirty years ago by Bourrely, Soffer and Wu to describe pp and $p\bar{p}$ elastic scattering beyond the GeV [7–9]. In the TeV domain, the scattering amplitude is written as in Eq. (3)

$$\mathcal{M}(s,t) = \frac{is}{2\pi}\int d^2\vec{b}\, e^{-i\vec{q}\cdot\vec{b}}\left(1 - e^{-\Omega(s,\vec{b})}\right), \tag{6}$$

where $\Omega(s,\vec{b})$ is related to the eikonal phase.

One of the main features of the model is the fact that s- and b-dependences in $\Omega(s,\vec{b}\,)$ are factorized as

$$\Omega\left(s,\vec{b}\right) = \mathcal{S}(s)\,F(b)\,. \tag{7}$$

The high-energy behaviour of $\mathcal{S}(s)$ is assumed to be given by

$$\mathcal{S}(s) = \frac{s^c}{(\log s)^{c'}} + \frac{u^c}{(\log u)^{c'}}\,, \tag{8}$$

where s and u are in GeV^2 and the approximation $\log u = \log s - i\pi$ is valid for the asymptotic behaviour at high energies.

The profile function $F(b)$ is obtained as a Fourier transform of $\tilde{F}(t)$, *i.e.*,

$$F(b) = \int_0^\infty dq\, q\tilde{F}\left(-q^2\right) J_0(q\,b)\,, \tag{9}$$

with

$$\tilde{F}(t) = fG^2(t)\frac{a^2+t}{a^2-t} \qquad \text{and} \qquad G(t) = \frac{1}{\left(1-t/m_1^2\right)\left(1-t/m_2^2\right)}\,, \tag{10}$$

where $G(t)$ is the electromagnetic form factor of the proton. This assumption means that the BSW model postulates that the charge distribution in the proton is related to the matter distribution.

In the BSW model, there are only six energy-independent parameters c, c', m_1, m_2, a and f that are given in Table I.

TABLE I

Parameters for the BSW model. Extracted from Ref. [8].

$c = 0.167$	$m_1 = 0.577$ GeV	$a = 1.858$ GeV
$c' = 0.748$	$m_2 = 1.719$ GeV	$f = 6.971$ GeV^{-2}

4. HEGS model

The High Energy General Structure (HEGS) model was developed by Selyugin [10,11] for the description of elastic pp and $p\bar{p}$ scattering, giving a quantitative description of the data in a wide energy range of $9.8 \leq \sqrt{s} \leq 8000$ GeV using a small number of fitting parameters. It uses the proton electromagnetic form factors calculated from the General Parton Distributions (GPDs) and assumes, similarly to the BSW model, that the matter distribution is proportional to the charge distribution on the proton.

The hadronic amplitudes are calculated through a unitarization procedure and are written, similarly to Eqs. (3) and (6), in the form of

$$F_H(s,t) = \frac{is}{2\pi}\int d^2\vec{b}\, e^{-i\vec{q}\cdot\vec{b}}\left(1 - e^{\chi\left(s,\vec{b}\right)}\right) \tag{11}$$

with the correspondence $\Omega(s,\vec{b}\,) = -\chi(s,\vec{b}\,)$ (see Eq. (7)). The microscopic contributions are taken into account in t-space through so-called Born terms $F_h^{\rm Born}(s,t)$, which are used to form the complex quantity

$$\chi(s,b) = \frac{i}{2\pi}\int d^2q\, e^{i\vec{b}\cdot\vec{q}}\, F_h^{\rm Born}\left(s,-q^2\right) . \tag{12}$$

The Born amplitude, in the extended version [11] of the model, is written as the sum of three main contributions, two cross-even parts and one possible odderon term

$$\begin{aligned} F_h^{\rm Born}(s,t) \;=\; & h_1\, F_1^2(t)\, F_a(s,t)\left(1 + \frac{R_1}{\hat{s}^{0.5}}\right) \\ & + h_2\, A^2(t)\, F_b(s,t) \\ & \pm h_{\rm odd}(t)\, A^2(t)\, F_b(s,t)\left(1 + \frac{R_2}{\hat{s}^{0.5}}\right) , \end{aligned} \tag{13}$$

where the $+\,(-)$ sign is used to compute pp ($p\bar{p}$) scattering and

$$h_{\rm odd}(t) = i\, h_3\, t/\left(1 - r_0^2\, t\right) . \tag{14}$$

The first two terms in Eq. (13) are interpreted by the author, respectively, as a possible Pomeron and a cross-even part of non-perturbative three gluon exchange. There may also be added a fourth contribution due to spin-flip, which is not relevant in the high-energy domain and is not included here. $F_1(t)$ and $A(t)$ are hadronic form factors, parametrized as

$$\begin{aligned} F_1\left(-q^2\right) \;&=\; \frac{4m_p^2 + \mu\, q^2}{4m_p^2 + q^2}\left(\frac{1}{1 + q/a_1 + q^2/a_2^2 + q^3/a_3^3}\right)^2 , \\ A\left(-q^2\right) \;&=\; \frac{\Lambda^4}{\left(\Lambda^2 + q^2\right)^2} , \end{aligned} \tag{15}$$

where $m_p = 0.93827$ GeV is the proton mass; $F_a(s,t)$ and $F_b(s,t)$ are Regge-like terms

$$F_a(s,t) = \hat{s}^{\,\epsilon}\, e^{B(s,t)\,t} , \qquad F_b(s,t) = \hat{s}^{\,\epsilon}\, e^{B(s,t)\,t/4} \tag{16}$$

with the slope[1]

$$B\left(s,-q^2\right)=\left(\alpha+k\frac{q}{q_0}e^{-k\,q^2\log\hat{s}}\right)\log\hat{s}\,, \tag{17}$$

where $q_0=1$ GeV and $s_0=4m_p^2$ set the momentum and energy scale.

The energy dependence appears here and in Eq. (13), through the complex quantity

$$\hat{s}=s\,e^{-i\pi/2}/s_0\,. \tag{18}$$

This last version of the HEGS model contains seven energy-independent fitting parameters, given in Table II. The parameters kept fixed are given in the same table. The fit is performed simultaneously in the data from the energy range of $9.8\leq\sqrt{s}\leq 8000$ GeV.

TABLE II

The first two rows show fitting parameters for the extended version of HEGS model. The second two rows give the fixed parameters in the data fit of the extended version of HEGS model. All these parameters are extracted from Ref. [11].

Fitted parameters			
$h_1=3.67$ GeV^{-2}	$h_2=1.39$ GeV^{-2}	$h_3=7.51$ GeV^{-4}	$k=0.16$ GeV^{-2}
$R_1=4.45$	$R_2=53.7$	$r_0^2=3.82$ GeV^{-2}	
Fixed parameters			
$a_1=16.7$ GeV	$a_2^2=0.78$ GeV^2	$a_3^3=12.5$ GeV^3	$\mu=2.79$
$\epsilon=0.11$	$\Lambda^2=1.6$ GeV^2	$\alpha=0.24$ GeV^2	

5. Discussion

Both BSW and HEGS models calculate the (s,t)-amplitudes in terms of the Fourier transform of eikonal functions $\Omega(s,\vec{b})$ and $\chi(s,\vec{b})$, as shown in Eqs. (6) and (11). The eikonals are related to the amplitude in the impact parameter representation of the KFK model (Eq. (1)) through

$$1-e^{-\Omega\left(s,\vec{b}\right)}=1-e^{\chi\left(s,\vec{b}\right)}=-\frac{i}{\sqrt{\pi}}\left[\tilde{T}_{\rm R}\left(s,\vec{b}\right)+i\,\tilde{T}_{\rm I}\left(s,\vec{b}\right)\right]\,. \tag{19}$$

The amplitudes $\tilde{T_K}(s,\vec{b})$ in b-space must fall fast with b, so that the integration can be performed numerically. They present oscillations for large $|q|$.

[1] The slope here does not refer to the traditional definition of the slope in the final hadronic amplitude responsible for the exponential behaviour at small t. Here, it accounts for non-linear aspects in the Regge-like terms $F_a(s,t)$ and $F_b(s,t)$ presented in the Born amplitude.

In the HEGS model, the integrands $(1 - e^{\chi(s,\vec{b})})$ are not additive contributions of the terms of the Eq. (13) and it is not easy to identify the influence term.

A comparison between the t-amplitudes is shown for 7 TeV in Fig. 1. Their normalization is understood as the differential cross section $d\sigma/dt$ and the total cross section $\sigma(s)$ are linked through

$$\frac{1}{(\hbar c)^2}\frac{d\sigma}{dt} = |T(s,t)|^2 = \frac{\pi}{s^2}|\mathcal{M}(s,t)|^2 = \frac{\pi}{s^2}|F_H(s,t)|^2\,, \tag{20}$$

$$\frac{\sigma_{\rm tot}(s)}{(\hbar c)^2} = 4\sqrt{\pi}\,T_{\rm I}(s,0) = \frac{4\pi}{s}\mathcal{M}_{\rm I}(s,0) = \frac{4\pi}{s}(F_H)_{\rm I}(s,0)\,. \tag{21}$$

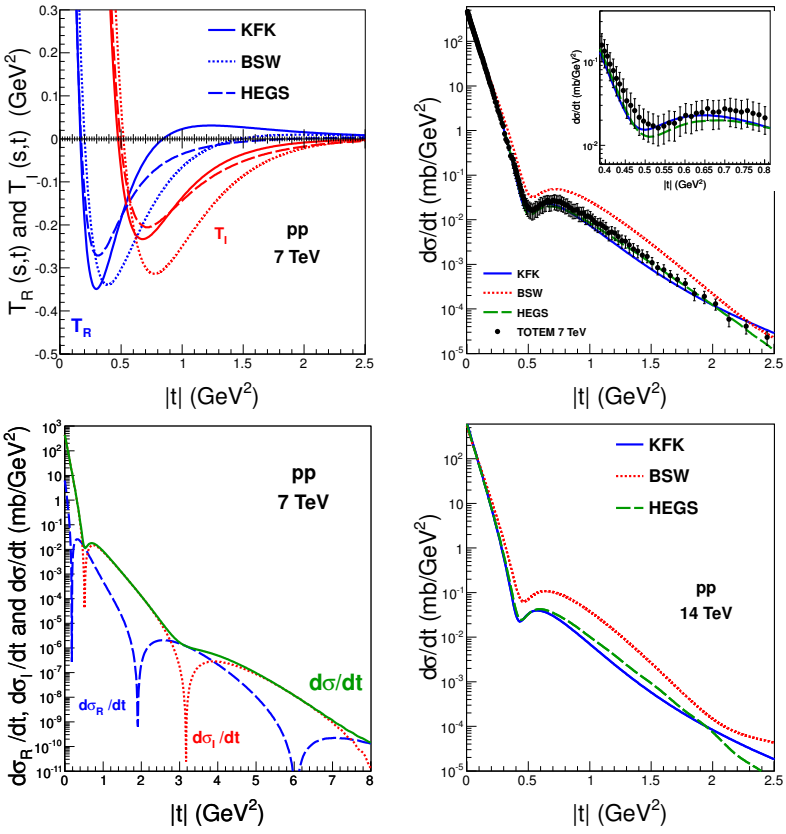

Fig. 1. Real and imaginary amplitudes (top left) and differential cross section (top right) of KFK (solid), BSW (dotted) and HEGS (dashed) models for $\sqrt{s} = 7$ TeV; differential cross section for HEGS model with imaginary and real contribution for $\sqrt{s} = 7$ TeV (bottom left), indicating the presence of a second zero in the imaginary amplitude, that does not occur in KFK; the differential cross section prediction for $\sqrt{s} = 14$ TeV (bottom right).

The Coulomb interaction is not included here. Figure 1 displays the differential cross section of the three models for 7 TeV compared to TOTEM data and the prediction for 14 TeV. Despite quite different microscopic construction, HEGS and KFK models describe well the available data and it is not possible to discriminate which one is in a better agreement with the data.

The magnitude of imaginary amplitudes in the plots between zeros are larger than the real magnitudes in the three models. These are oscillatory in $d\sigma/dt$ with dips near $T_{\rm I}$ zeros, as shown in Fig. 1 for the HEGS model. It will be difficult to confirm the oscillatory behaviour as they occur for large$-|t|$. In the KFK model, the amplitudes $T_{\rm R}(s,t)$ and $T_{\rm I}(s,t)$ in t-space have simpler analytical forms, with only one imaginary zero and two real zeros (at least for $|t| \sim 30$ GeV^2).

The similarities of KFK, BSW and HEGS models can only be described up to the location of the second real zero, namely up to $|t| \leq 3$ GeV^2 for $\sqrt{s} = 7$ TeV. Figure 2 shows the zeros of the real and imaginary amplitudes in the three models. We can note that the first real zero and the first imaginary zero are in very good agreement among the three models.

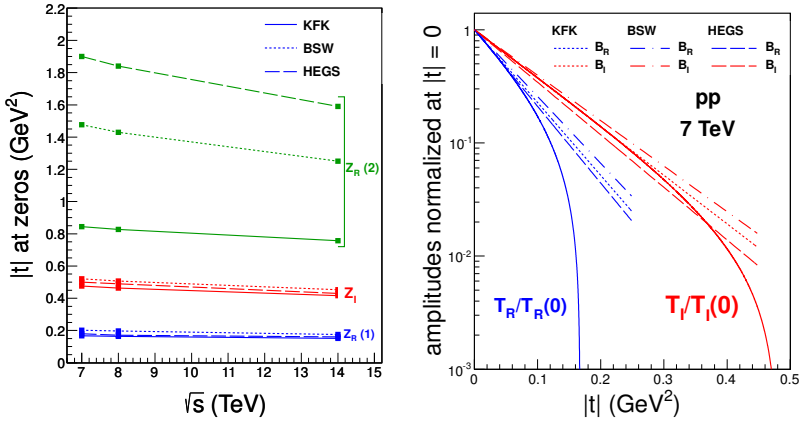

Fig. 2. Positions of zeros of the amplitudes of KFK, HEGS and BSW models as a function of energy (left); real and imaginary amplitude of the models for small $|t|$ for $\sqrt{s} = 7$ TeV, with the slopes at $t = 0$, stressing that $B_{\rm R} > B_{\rm I}$ in all cases.

A common feature of these three models with full $|t|$-description of the amplitudes is that, although the values of slopes of imaginary and real amplitudes at $t = 0$ are essentially different, they all agree $B_{\rm R} \neq B_{\rm I}$, in particular, $B_{\rm R} > B_{\rm I}$. This behaviour is shown in Fig. 2 and must be taken into account in the analysis of the forward scattering data for the estimates of the total cross sections $\sigma_{\rm tot}(s)$ and of the $\rho(s) = T_{\rm R}(s, t = 0)/T_{\rm I}(s, t = 0)$ quantities [12].

The authors wish to thank CNPq and FAPERJ for financial support.

REFERENCES

[1] G. Antchev *et al.* [TOTEM Collaboration], *Europhys. Lett.* **95**, 41001 (2011); **96**, 21002 (2011); **101**, 21002 (2013).

[2] G. Aad *et al.* [ATLAS Collaboration], *Nucl. Phys. B* **889**, 486 (2014).

[3] H.G. Dosch, E. Ferreira, A. Kramer, *Phys. Rev. D* **50**, 1992 (1994).

[4] A.K. Kohara, E. Ferreira, T. Kodama, *Phys. Rev. D* **87**, 054024 (2013); *Eur. Phys. J. C* **73**, 2326 (2013).

[5] A.K. Kohara, E. Ferreira, T. Kodama, *Eur. Phys. J. C* **74**, 3175 (2014).

[6] W. Faissler *et al.*, *Phys. Rev. D* **23**, 33 (1981).

[7] C. Bourrely, J. Soffer, T.T. Wu, *Phys. Rev. D* **19**, 3249 (1979); *Nucl. Phys. B* **247**, 15 (1984); *Eur. Phys. J. C* **28**, 97 (2003).

[8] C. Bourrely, J.M. Myers, J. Soffer, T.T. Wu, *Phys. Rev. D* **85**, 096009 (2012).

[9] C. Bourrely, *Eur. Phys. J. C* **74**, 2736 (2014).

[10] O.V. Selyugin, *Eur. Phys. J. C* **72**, 2073 (2012).

[11] O.V. Selyugin, *Phys. Rev. D* **91**, 113003 (2015); private communication is gratefully acknowledged.

[12] O.V. Selyugin, `arXiv:1310.0928 [hep-ex]`.